MACHINE-INDUCED BACKGROUNDS: THEIR ORIGIN AND LOADS ON ATLAS/CMS*

N.V. Mokhov#, FNAL, Batavia, IL 60510, U.S.A.
T. Weiler, CERN, Geneva, Switzerland

Abstract

A detailed analysis of machine-induced backgrounds (MIB) in the LHC collider detectors is performed with focus on origin and rates for three sources: tertiary beam halo, beam-gas interactions and kicker prefire. Particle fluxes originating from these operational and accidental beam losses are carefully calculated with the MARS15 code and presented at the entrance to the ATLAS and CMS experimental halls. It is shown that background rates in detector subsystems strongly depend on the origin of MIB, particle energy and type. Using this source term, instantaneous and integrated loads on the detectors and impact on the detector performance can be derived.

INTRODUCTION

The overall detector performance at the LHC is strongly dependent on the background particle rates in detector components. Particles originating from the interaction point (IP) are thought to be the major source (>99%) of background and radiation damage in the ATLAS and CMS detectors at nominal parameters and with a well tuned machine. Beam loss in the IP vicinity is the second source of background, but minor at nominal conditions [1, 2]. Particle fluxes generated by such beam interactions are called machine-induced backgrounds (MIB). As shown in [2], the relative importance of this component can be comparable to the first one at early operation of the LHC because MIB is mostly related to beam intensity and not luminosity, and tuning of the LHC will require substantial time and efforts. These facts are confirmed by the Tevatron experience.

Even in good operational conditions in an accelerator, some particles leave the beam core – due to various reasons [3] - producing a beam halo. Particle fluxes, generated in showers developed at halo interactions with limiting apertures, are responsible for MIB rates and radiation loads in accelerator and detector components. A multi-stage collimation system reduces these rates at critical locations by orders of magnitude; e.g., a factor of 10^3 at the Tevatron [3]. In addition to these slow losses, there is a probability of fast single-pass losses, caused, e.g., by an abort kicker prefire, when a certain number of bunches can make it through an unprotected section of the ring and be lost in front of the detector. Impact on the machine and collider detectors can be quite severe [4]. Tertiary collimators - as the last line of defense for slow and fast beam losses in the IP vicinity - are mandatory in the LHC, as proven at the Tevatron.

*Work supported by Fermi Research Alliance, LLC, under contract No. DE-AC02-07CH11359 with the U.S. Department of Energy.
#mokhov@fnal.gov

In this paper, a description of three terms of MIB is given. The proton losses on the IP1 and IP5 tertiary collimators are calculated using a collimation version of SixTrack [5]. Beam-gas interaction modeling as well as comprehensive simulation of hadronic and electromagnetic showers induced in the LHC components are performed with the 2008 version of the MARS15 code [6]. All essential details of the machine, interface, detectors and conventional constructions in ±550-m regions of IP1 and IP5 are taken into account: 3-D geometry, materials, magnetic fields, tunnel and rock outside (up to 12-m radially). Note that the code and approach were successfully benchmarked over 15 years at the Tevatron and DØ and CDF collider detectors. Particle fluxes above 20 MeV at the interface scoring plane at z=22.6m from the IP are calculated for further tracking in the ATLAS and CMS detectors. Representative distributions are shown, with respective source term files available to the detector collaborations.

MIB SOURCES IN IP1 AND IP5

1. Collimation Tails ("tertiary beam halo")

The first term of MIB for the experiments are protons escaping the betatron and momentum cleaning insertions (IP7 and IP3, respectively) and being intercepted by the tertiary collimators TCT. This term, related to the inefficiency of the main collimation system, is called "tails from collimators" or "tertiary beam halo". The TCTs are situated between the neutral beam absorber (TAN) and D2 separation dipole at about 148m on each side of IP1 and IP5. It is noted that most of protons coming from IP3 and IP7 would be lost in the triplet (closer to the experiment) if they were not intercepted by the TCTs. Assuming an ideal machine (no alignment and magnet errors) at 7 TeV and the high-luminosity insertions (IP1 and IP5) squeezed to $\beta^* = 0.55$m, we only take into account the contribution from the betatron cleaning in IP7 at the rate of 8.3×10^9 p/s for a 10-hr beam lifetime and nominal intensity. The collimators were set to the nominal settings, in this case 8.3σ for the tertiary collimators, to fully protect the triplet magnets. The resulting loss rates on the TCTs are 2.61×10^6 p/s and 4.28×10^6 p/s for Beam-2 approaching IP5 and Beam-1 approaching IP1, respectively. Corresponding loss rates on the other sides of these insertions are about 10% of those. 95% of muons illuminating ATLAS and CMS in a radius of 3m are generated at 50<z<148m from the IP. Note that the above rates are ~45 times higher for the transient 0.22-hr beam lifetime. Contributions from the momentum cleaning are thought to be substantially lower.

2. Beam-Gas Interactions

Beam-gas interactions [7, 8] comprise the second term of MIB. Products of beam-gas interactions in straight sections and arcs upstream of the experiments and not intercepted by the collimation system have a good chance to be lost on limiting apertures in front of the collider detectors. As described in [7, 8], the main process of beam-gas interaction, multiple Coulomb scattering, results in slow diffusion of protons from the beam core causing emittance growth. These particles increase their betatron amplitudes gradually during many turns and are intercepted by the main collimators before they reach other limiting apertures. Similar behaviour takes place for small-angle elastic nuclear scattering. In inelastic nuclear interactions, leading nucleons and other secondaries are generated at angles large enough for them to be lost within tens or hundreds of meters of the LHC lattice after such interactions.

The rate of beam-gas interactions is proportional to the beam intensity and residual gas pressure in the beam pipe. Longitudinally it follows the pressure maps of [9]. The points of beam interactions with residual gas nuclei can be sampled from these maps for the given operational conditions [10], using corresponding lattice functions. At the nominal beam current, the expected rates of inelastic nuclear interactions (m^{-1} s^{-1}) in IP1 and IP5 are about 10 in the UX detector region, 400 in the inner triplet and cold segments of the matching section, 20-30 in the warm sections in-between, and 8×10^3 in the arcs [11]. Detailed studies since the first papers on MIB in LHC [1, 2] have shown that inelastic and large-angle elastic nuclear interactions in the 550-m regions upstream of IP1 and IP5 are mostly responsible for the beam-gas component of MIB Fig. 1). The total number of elastic and inelastic nuclear interactions in these regions for each of the beams coming to IP1 and IP5 is 3.07×10^6 p/s which is used for normalization in this paper. Despite a high gas pressure – and beam-gas interaction rate – in the arcs, most muons coming to ATLAS and CMS are generated in ±400-m regions around IP1 and IP5. The others are absorbed/scattered in the magnets and rock (especially that tangent to the orbit).

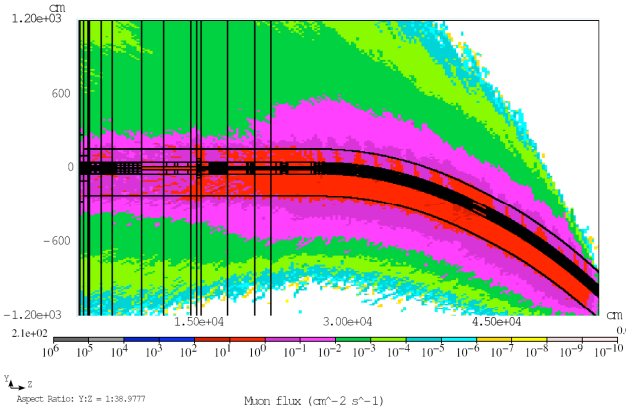

Figure 1: Muon flux isocontours in the orbit plane at 22<z<550m upstream IP1 and IP5.

At certain conditions, an additional contribution can come from medium-angle elastic scattering [8]. Such a process can result in a substantial increase of the betatron amplitude and, if not intercepted by the main collimators, the scattered protons can be lost in the vicinity of the experimental insertions. This single-pass process, taking place between the cleaning insertions and 550-m regions around IP1 and IP5, can give some rise to the "scraping" rate on the TCTs adding to MIB.

3. Kicker Prefire

The third term of MIB is generated by remnants of a mis-steered beam uncaptured in the IP6 beam dump system. These irregular fast losses are caused by machine failures, such as irregular dumps. As was first shown in [4], the impact on the machine and collider detectors – without a multi-component protection system in IP6 [12] - can be disastrous. The worst design case is a dump kicker module prefire. If such an event is detected, the remaining 14 modules will be fired within 700ns to dump the beam [13]. Since the dump kicker modules need a certain time to reach their nominal strength (~3μs), a certain number of bunches will be deflected before they are extracted at the end of one turn.

The scenario considers a kicker prefire, assuming a π/2 phase advance between the pre-firing kicker magnet and the TCT tertiary horizontal collimator in front of IP5 (worst case). This results in maximum deflection of the beam at the location of the TCT [14]. Furthermore it is assumed that the dump protection is misaligned so that protons with a betatron amplitude between 8.3σ (nominal setting of the collimator at 7TeV and β* = 0.55m in IP5) and 10σ will hit the TCTs.

Our calculations have shown that some protons of 8 mis-steered bunches of Beam 2, separated by 25 ns and each of 1.15×10^{11} protons, can hit the IP5's TCT. The total amount of protons deposited on the TCT is of the order of 2 to 2.5 full bunches. Particles with a deflection below 5.08σ (μrad) pass through IP5 and may hit the IP7 collimators or are extracted after one turn, while those with a deflection above 10.28σ (μrad) are all assumed to be absorbed by the IP6 dump system (Fig. 2).

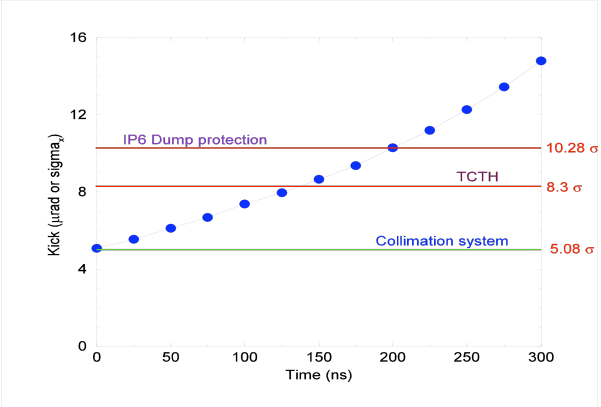

Figure 2: Angular kick for 13 bunches at prefire of the MKD.OR6.B2 beam dump kicker module.

BEAM 2 MIB ON CMS

In this section, side-by-side comparison is given for various distributions of particles crossing the z=22.6m plane and approaching the IP5 with Beam 2 towards CMS, i.e., counter-clockwise. MARS15 results for hadrons, muons, photons and electrons above 20 MeV are presented for the nominal conditions and are normalized to cm^{-2} s^{-1} for the tertiary halo and beam-gas cases, and to cm^{-2} per accident for kicker prefire. The distributions cover laterally the entire detector: inner tracker, forward and barrel calorimeters, and muon chambers.

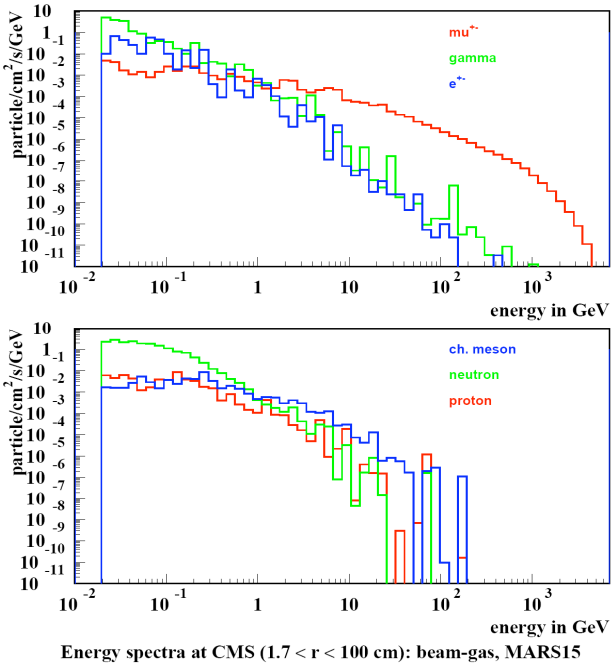

Energy spectra at CMS (1.7 < r < 100 cm): beam-gas, MARS15

Figure 3: Particle energy spectra at z=22.6 m from IP5 in the 1.7 < r < 100cm region for beam-gas.

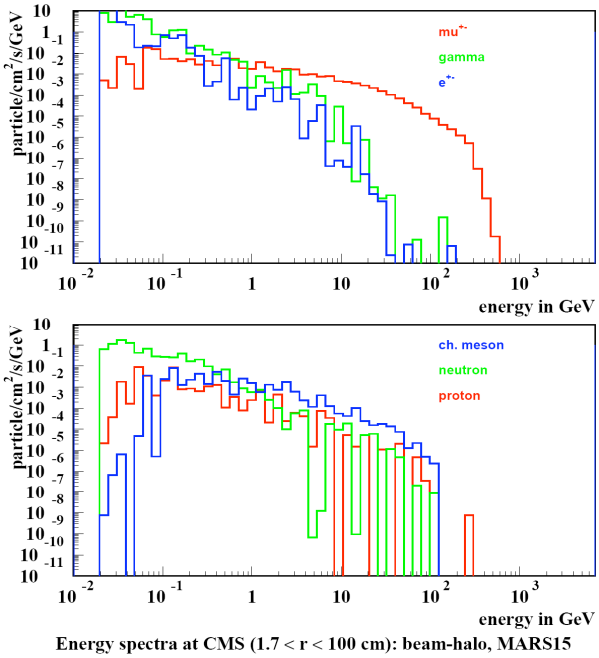

Energy spectra at CMS (1.7 < r < 100 cm): beam-halo, MARS15

Figure 4: Same as in Fig. 3, for tertiary halo.

Figs. 3 and 4 show particle energy spectra at 1.7<r<100cm for beam-gas and tertiary halo, respectively. The spectra are not very different for the two sources, but muons up to 5 TeV are present for beam-gas while there are no muons above 0.6 TeV induced by beam losses on the TCT collimators (much shorter decay path in the later case). At energies below 1 GeV, particles other than muon dominate. Radial distributions are shown in Figs. 5 and 6. The distributions are not that different for the two sources at r < 3 m, but at larger radii they are pretty flat for beam-gas and drop rapidly (except neutrons) for tertiary halo.

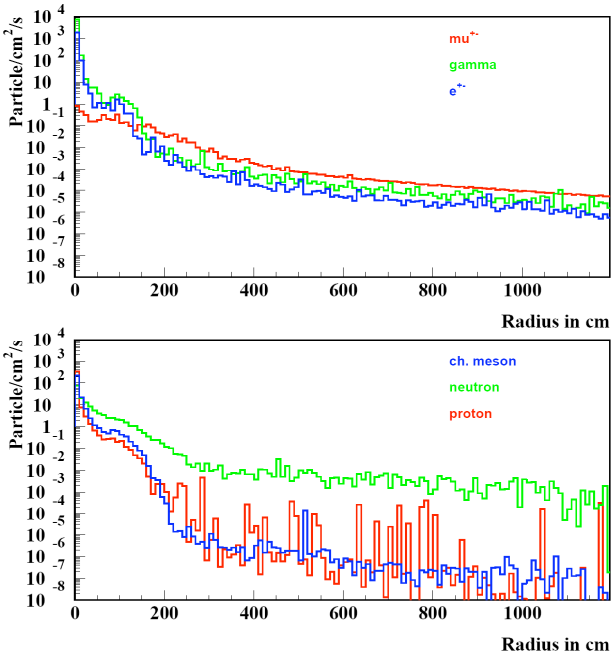

Radial distributions at CMS (E > 0.02 GeV): beam-gas, MARS15

Figure 5: Radial distributions of particle fluxes (E>20 MeV) at z=22.6 m from IP5 for beam-gas.

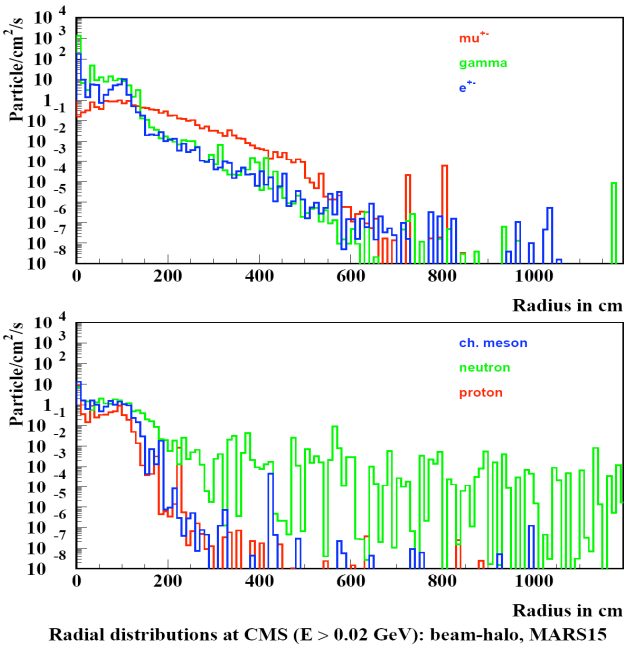

Figure 6: Same as in Fig. 5, for tertiary halo.

Muon energy spectra in four radial regions are shown in Figs. 7 and 8 for beam-gas and tertiary halo, respectively. As noted above, spectra for beam-gas outside of the beam pipe are much harder compared to those for tertiary halo and kicker prefire (as will be shown later). There are almost no charged particles at r>6m for the latter two sources. The peak muon flux at the ATLAS and CMS detectors for beam-gas and tertiary halo is about 1 $cm^{-2}s^{-1}$.

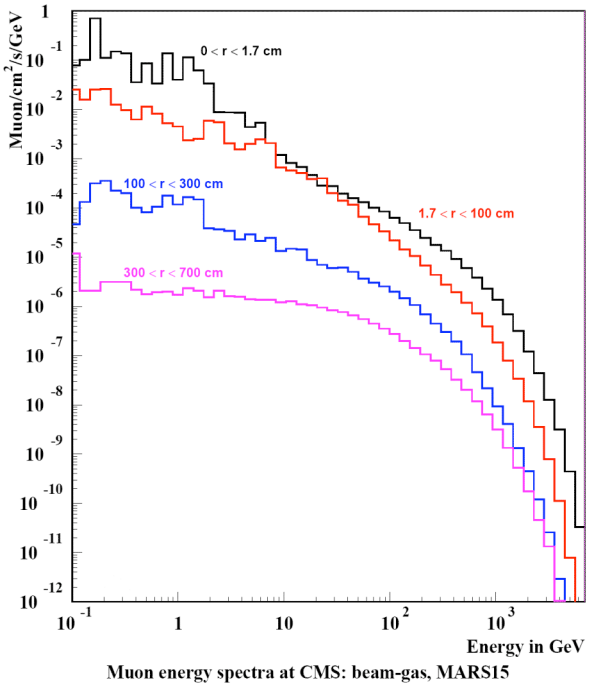

Figure 7: Muon energy spectra at z=22.6 m from IP5 in 4 radial regions for beam-gas.

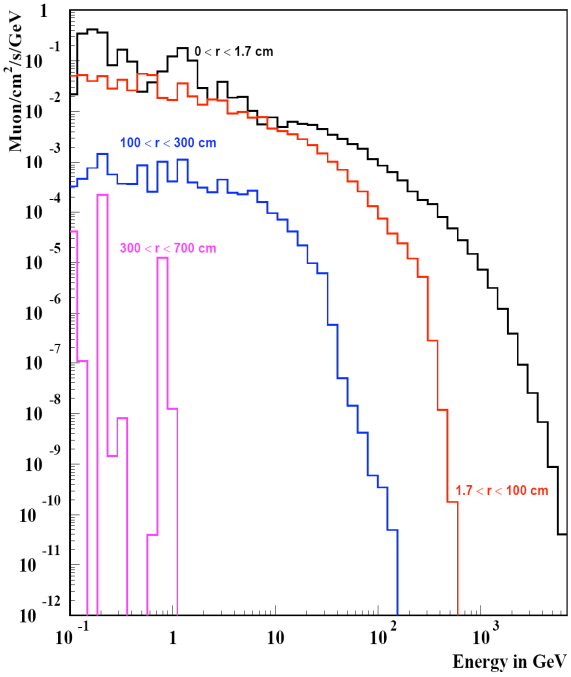

Figure 8: Same as in Fig. 7, for tertiary halo.

The difference between the two sources is further illustrated in Figs. 9 and 10. Beam-gas interactions – contributing to muon fluxes on ATLAS and CMS – take place up to 500m upstream of the IP1 and IP5, respectively, which results in the presence of very energetic muons through the entire detector cross-section.

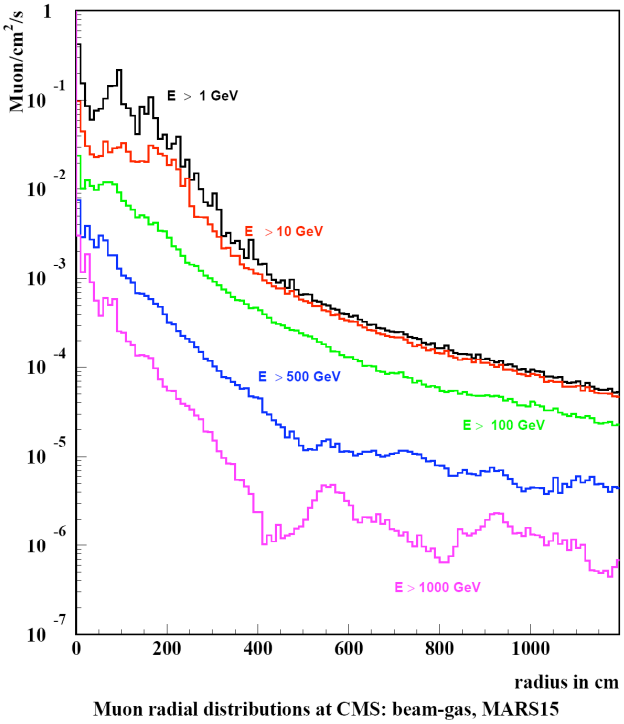

Figure 9: Radial distributions of muon fluxes above 5 cut-off energies at z=22.6 m from IP5 for beam-gas.

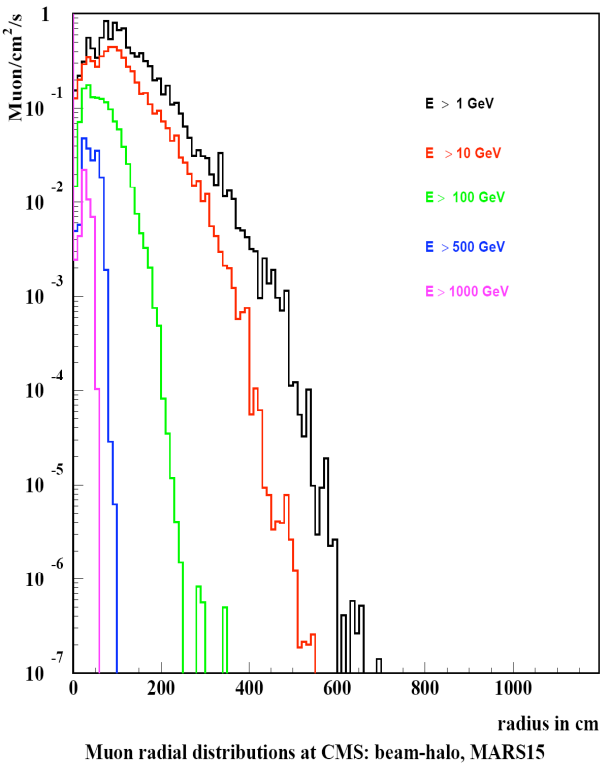

Figure 10: Same as in Fig. 9, for tertiary halo.

Muon fluxes, resulting from beam-gas interactions, exhibit rather strong vertical/horizontal and left/right asymmetry (see Fig. 1), certainly at distances greater than 2 meters from the beam axis, as shown in Fig. 11. This is also true for other particles – photons and electrons first of all – accompanying the muons. Contrary, particle flux distributions at the detectors (outside the beam pipe) from tertiary halo and kicker prefire are pretty symmetric around the beam axis at IP1 and IP5. This is because of the point-like nature of the source (TCT) and just a straight section between that source and the detector.

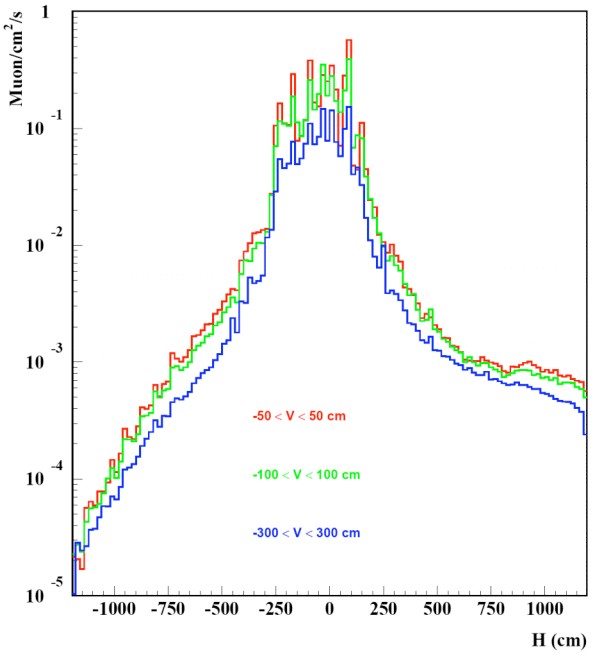

Figure 11: Horizontal distributions of muon fluxes in 3 vertical slices at z=22.6 m from IP5 for beam-gas.

SUM RULES FOR MIB IN ATLAS/CMS

The previous section gives detailed information on beam-gas and tertiary halo contributions to the MIB in CMS for the counter-clockwise Beam 2. The MARS15 results presented can be used with a good – from a practical standpoint – accuracy for estimation of the total MIB loads on ATLAS and CMS. The sum rules are especially accurate for the energetic muon component.

Let's define the beam-gas results presented above as BG, and tertiary halo results for the betatron cleaning of Beam 2 in IP5 as BH. Proton losses for the betatron cleaning have been calculated with SixTrack and their rate on the IP1 and IP5 tertiary collimators gives us corresponding weighting factors for the total loss. Thus, the total MIB stationary load on ATLAS is estimated as (BG+0.12 BH) on the right side (Beam 1) and (BG+1.64BH) on the left side (Beam 2). For CMS, the corresponding rules are (BG+BH) on the right side (Beam 2) and (BG+0.085BH) on the left side (Beam 1), which gives about 3 muons/cm^2/s for the maximum total muon flux at the detector center.

KICKER PREFIRE

This section gives results for the third component of MIB, generated by remnants of a mis-steered beam uncaptured in the IP6 beam dump system. As with the first two sources, particle fluxes above 20 MeV are calculated with MARS15 at the interface plane z=22.6 m for the counter-clockwise Beam 2 approaching CMS. It was found in our calculations that mainly protons from bunch 4 through 9 hit the TCT to the load on CMS in the case considered (Figs. 12 and 13).

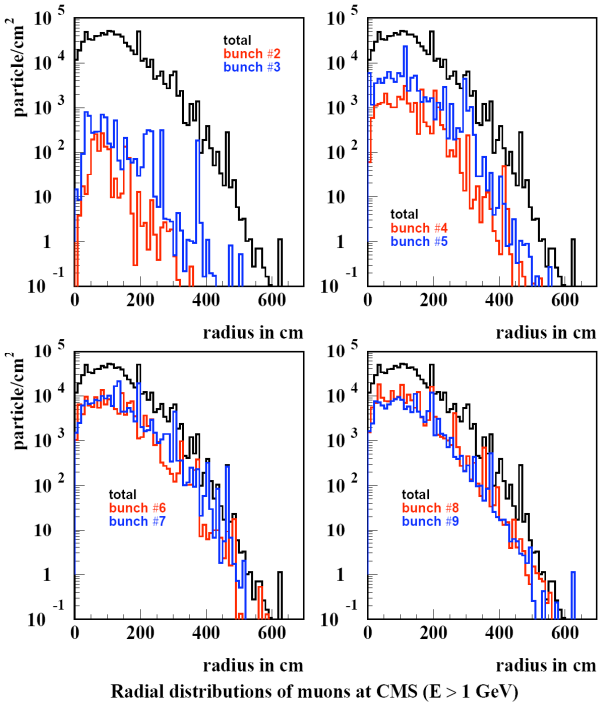

Figure 12: Radial distributions of muon fluxes above 1 GeV at z=22.6 m from IP5 for a kicker prefire event: total and for bunches 2 through 9.

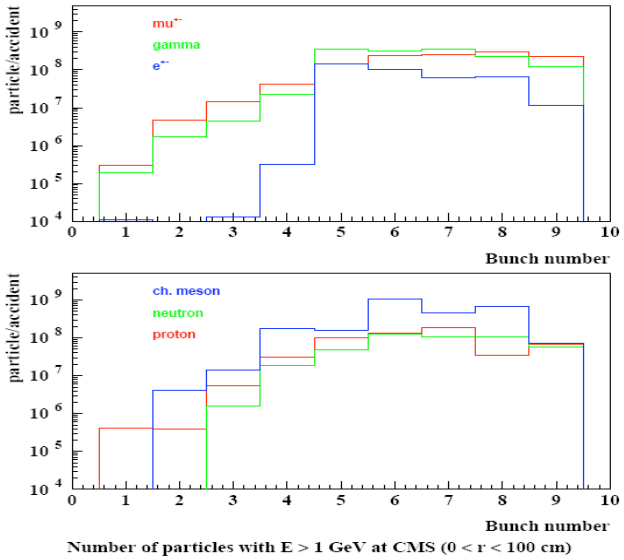

Figure 13: Bunch distribution for particle load on CMS (E> 1 GeV, r < 100 cm).

Fig. 14 shows energy spectra of particles approaching the CMS detector in the first meter radially outside the TAS aperture of 1.7 cm. General features of the spectra are similar to those with two other sources. It is interesting to note the presence of rather energetic tails for hadrons and muons more energetic than for tertiary halo because of more grazing-angle events on the TCTs.

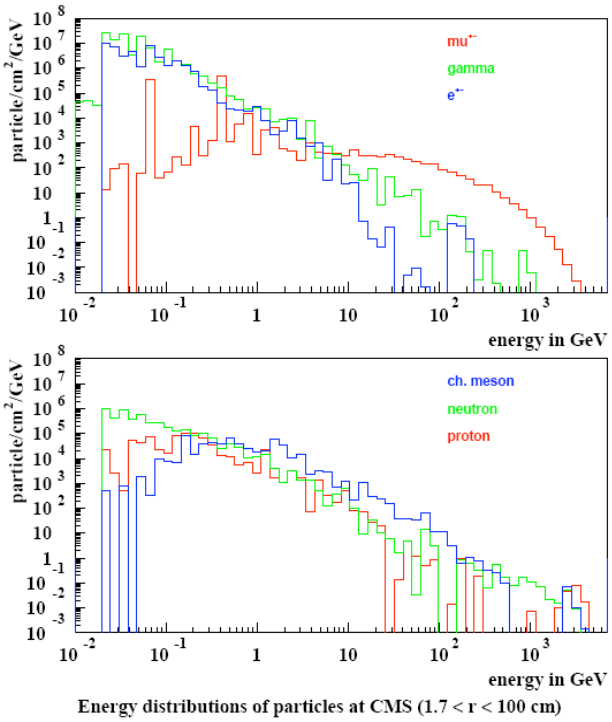

Figure 14: Particle energy spectra at z=22.6 m from IP5 in the 1.7 < r < 100cm region for kicker prefire.

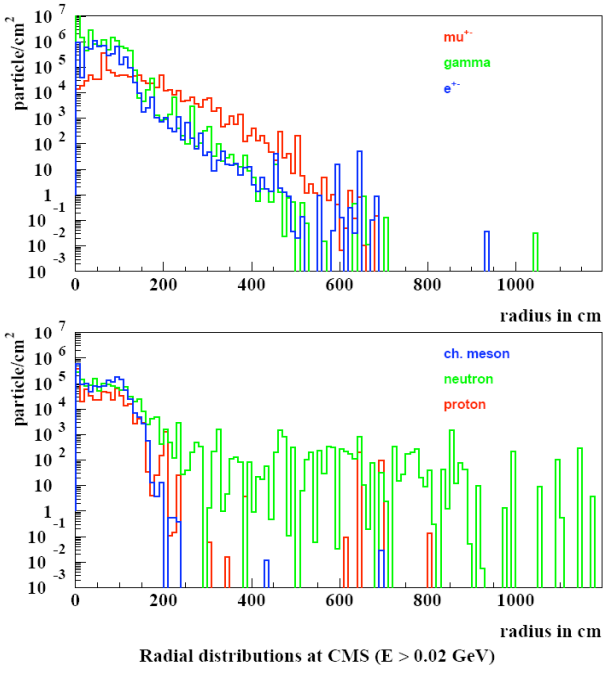

Figure 15: Radial distributions of particle fluxes (E>20 MeV) at z=22.6 m from IP5 for kicker prefire.

Radial distributions of particle fluxes above 20 MeV and muon fluxes for 5 cut-off energies from 1 GeV to 1 TeV are shown in Figs. 15 and 16, respectively. Again, they are not that different from the tertiary halo case. Temporal considerations though are quite different: a continuous steady state for the beam-gas and tertiary halo

cases, and a very short 125-150 ns pulse for the case of kicker prefire. As a result, the integral loads from a kicker prefire event are very small compared to all other sources, while large instantaneous ionization over all the detector volume can cause irreversible damage by creating breakdown in some components [4]. Estimated peak dose and MIP flux for the innermost CMS pixel are about 0.02 Gy and 10^8 cm^{-2} per such an event. Note that the loads induced by a kicker prefire are much lower for Beam 1 at CMS and for both beams on ATLAS compared to those considered here for Beam 2.

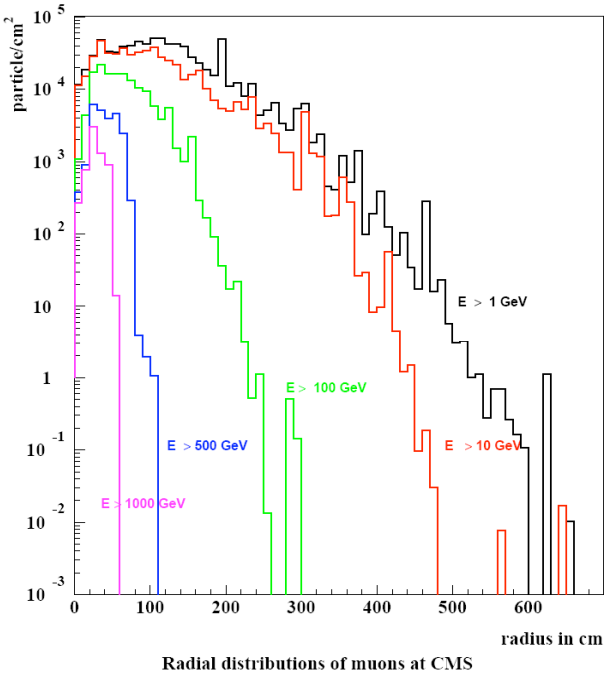

Figure 16: Radial distributions of muon fluxes above 5 cut-off energies at z=22.6 m from IP5 for kicker prefire.

CONCLUSIONS

Detailed MARS15 calculations of machine-induced backgrounds have been performed for the current models of the LHC high-luminosity insertions, gas pressure, steady state and fast beam losses in the vicinity of IP1/IP5. Results presented are consistent with our earlier results of the mid-90s. Tertiary collimators protect critical detector components at beam accidents, and reduce steady state machine backgrounds at small radii. The sum rules for calculation of total MIB loads have been derived for the ATLAS and CMS detectors. The files of particles at the interface plane z=22.6m are available to the detector community; several groups have already started corresponding detector modeling.

Thanks to A. Rossi and M. Huhtinen for crucial input to a gas pressure model and S. Striganov for help with enhancement of the analysis tools.

REFERENCES

[1] N.V. Mokhov, Nucl. Physics B, 51A (1996) 210.
[2] A.I. Drozhdin, M. Huhtinen, N.V. Mokhov, Nucl. Instr. And Meth. A381 (1996) 531.
[3] N.V. Mokhov, "Beam Collimation at Hadron Colliders", AIP Conf. Proc. 693, p. 14 (2003).
[4] A.I. Drozhdin, N.V. Mokhov, M. Huhtinen, "Impact of the LHC Beam Abort Kicker Prefire on High Luminosity Insertion and CMS Detector Performance", Proc. PAC'99, p. 1231, New York, 1999; Fermilab-Conf-99/060 (1999).
[5] G. Robert-Demolaize, et al., "A New Version of SIXTRACK with Collimation and Aperture Interface", PAC'05, Knoxville, Tennessee, 2005.
[6] N.V. Mokhov, "The Mars Code System User's Guide", Fermilab-FN-628 (1995); N.V. Mokhov, S.I. Striganov, "MARS15 Overview", in *Proc. of Hadronic Shower Simulation Workshop*, Fermilab, September 2006, AIP Conf. Proc. 896, p. 50 (2007); Fermilab-Conf-07/008-AD (2007); http://www-ap.fnal.gov/MARS/
[7] N.V. Mokhov, V.I. Balbekov, "Beam and Luminosity Lifetime", in *Handbook of Accelerator Physics and Engineering, 2nd Printing*, Ed. A.W. Chao, M. Tigner, P. 218, World Scientific (2002).
[8] A.I. Drozhdin, V.A. Lebedev, N.V. Mokhov et al., "Beam Loss and Backgrounds in the CDF and D0 Detectors due to Nuclear Elastic Beam-Gas Scattering", PAC'03, Portland, Oregon, 2003; also Fermilab-FN-734 (2003). http://www.JACoW.org.
[9] A. Rossi, CERN-LHC-Project-Report 783 (2004).
[10] M. Huhtinen, private communication.
[11] M. Huhtinen, these proceedings.
[12] N.V. Mokhov, A.I. Drozhdin, I.L. Rakhno, M. Gyr, E. Weisse, "Protecting LHC Components against Radiation Resulting from an Unsynchronized Beam Abort", Proc. PAC'01, p. 3168, Chicago, 2001; Fermilab-Conf-01/133 (2001).
[13] The LHC Collaboration, "LHC Design Report, Volume1", CERN-2004-003-V1, 2004.
[14] R. Assmann, et. al., "The Consequences of Abnormal Beam Dump Action on the LHC Collimation System", LHC-Project-Note-293, 2002.